ADIPEC 0911

Predictive modelling of naturally fractured reservoirs using geomechanics and flow simulation

Stephen J. Bourne[1], Franz Brauckmann[2], Lex Rijkels[1], Ben J. Stephenson[1], Alex Weber[2] and Emanuel J.M. Willemse[1]; [1]Shell International, The Hague, [2]BEB, Hannover

This paper was selected for presentation at the 9th Abu Dhabi International Petroleum Exhibition and Conference held in Abu Dhabi, U.A.E., 15-18 October 2000.

Abstract

To optimise recovery in naturally fractured reservoirs, the field-scale distribution of fracture properties must be understood and quantified. We present a semi-deterministic method to systematically predict the spatial distribution of natural fractures and their effect on flow simulations. This approach enables the calculation of field-scale fracture models. These are calibrated by geological, well test and field production data to constrain the distributions of fractures within the inter-well space.

First, we calculate the stress distribution at the time of fracturing using the present-day structural reservoir geometry. This calculation is based on geomechanical models of rock deformation such as elastic faulting. Second, the calculated stress field is used to govern the simulated growth of fracture networks. Finally, the fractures are upscaled dynamically by simulating flow through the discrete fracture network per grid block, enabling field-scale multi-phase reservoir simulation. Uncertainties associated with these predictions are considerably reduced by constraining and validating the models with seismic, borehole, well test and production data.

This approach is able to predict physically and geologically realistic fracture networks. Its successful application to outcrops and reservoirs demonstrates there is a high degree of predictability in the properties of natural fracture networks. Several examples show the success of the method in single- and multi-phase fields. In cases of limited data – where stochastic models typically fail - this method remains robust.

Introduction

Natural fracture systems can have a dramatic impact on reservoir performance - they may act as highly permeable flow conduits or act as baffles and seals. The complexity of a fracture network typically leads to an extremely heterogeneous and anisotropic permeability distribution within the reservoir. Successful management of these reservoirs is impossible without substantial knowledge of the natural tensile and shear fracture systems. It is essential to know their spatial distribution and hydraulic properties on an inter-well scale to properly simulate the field-wide recovery processes.

This paper presents a new method for predicting natural fracture distributions and their effect on reservoir simulations (Figure 1). The first step uses geomechanical models of rock deformation to calculate the field-scale distribution of stress responsible for fracturing from the observed structural geometry of the field. Fracture network geometries are then obtained by simulating the initiation, growth, and termination of fractures within the calculated stress field. These predicted network geometries are partially constrained and validated by core, borehole image, mud loss, and outcrop data. Thereafter, multi-phase, well-scale or field-scale flow simulations of the fracture model are validated and calibrated against well test and production data.

Close integration of fracture prediction and flow simulation enables significant reductions in uncertainty by using all the available static and flow data to constrain a single model. In this way, for instance, standard ambiguities in borehole fracture data due to sampling bias can be overcome by the use of well inflow data. Moreover, as the fracture model is field-scale, the greater the number of wells available the smaller the uncertainty in fracture prediction becomes across the whole field and not just around the wells. Such reduction in uncertainty allows improved field development through: (i) better assessment of the recovery mechanism, (ii) more reliable production forecasts, (iii) well placement for optimal drainage, (iv) minimal water-cut, and (v) recognition of drilling hazards associated with fractures.

The following sections describe how structural geometry is used to predict stress, how stress is used to predict fractures, and how fractures are used to predict flow. We finish by presenting two applications of this method to producing carbonate reservoirs.

2. Fracture prediction

It is neither possible nor generally necessary to accurately predict individual fractures within a reservoir. Rather, we restrict our attention to predicting just the properties of those tensile and shear fracture networks that are hydraulically conductive. We calculate the stress field responsible for reservoir fracturing using geomechanics. Brittle fractures form where this stress field exceeds the local material strength as characterised by the brittle failure envelope for both tensile and shear fractures.

Continuum mechanical models. We consider deformation of the reservoir to be distributed smoothly on length-scales of interest. In this way we can combine knowledge of the regional stress history and the mean rock strength to calculate a smooth field of stress. Large discontinuities in the deformation field, such as seismically visible faults must be represented in the model explicitly rather than as part of the continuum.

The simplest approach to determine the stress field within a faulted reservoir is to assume the rocks behave as a homogeneous, isotropic, and linear-elastic material, and the faults as surfaces free of shear stress. In this model large-scale mechanical heterogeneity is represented only in the form of three-dimensional fault geometries.

The distribution of elastic stress related to faulting is governed by the distribution of slip over the fault network. However, fault displacements cannot, in general, be observed with sufficient precision, and even then only the dip-slip component of the fault offset. Hence no reliance is placed on observed fault displacements. Instead, we calculate the distribution of slip over the fault network by loading it according to the remote stress that caused the faults to slip. The orientation of this remote stress is estimated from the regional geological history, and the magnitudes according to the mean rock strength prior to faulting. A unique pattern of fault slip exists which releases all shear stress resolved onto the faults by the remote stress and other nearby faults. Such a slip distribution represents the static equilibrium of faults that possess zero shear strength. This is a reasonable approximation given that the residual shear strength of faults is typically at least ten times less than the strength of rock between the faults.

Numerical solutions for the elastic stress field are obtained using a three-dimensional boundary element analysis called Poly3D[1]. Poly3D solves the equations of linear elasticity by representing fault surfaces with a series of triangular elements, each of constant slip[2,3]. This approximation permits solutions for complicated three-dimensional fault geometries and slip distributions by using a large number of triangles to represent the often irregular fault geometries found in seismic data. Previous applications of elastic faulting models to geological problems include: fault interaction[4,5], fault growth[6-9], fault linkage[10,11], and fault-related fracturing[12-14].

Figure 2 illustrates the distribution of elastic stress calculated for a simple hypothetical network of right-lateral strike-slip faults. Notice the characteristic mean stress reduction in areas just to one side of the fault tips, e.g. at (–400, 1400), where rocks have been stretched by moving along the fault plane away from the fault tip. This causes tensile fractures which propagate at high angles away from the fault in the direction of greatest compression (c.f. Figure 3). Elsewhere the stress field is more complex and defies simple intuition. This is a consequence of mechanical interaction between faults so closely spaced that their stress fields overlap, e.g. at (200, 1000).

Faulting is typically the primary mechanism for the accommodation of strain within deforming brittle rocks. Therefore simple elastic faulting models are expected to be sufficient for fracture prediction in many structural settings. The remainder of this paper will focus on fracture prediction around faults and conclude by presenting two applications of this predictive model to producing carbonate reservoirs.

Brittle-elastic failure models. The fault-related stress fields calculated by Poly3D are wholly elastic, and therefore no allowance is made for stress relaxation that follows secondary fracture formation around faults. This approximation remains reasonable if the secondary fractures are small in size compared to the primary faults. In this case individual fractures will induce only small perturbations on the elastic stress field, which can be neglected. The elasticity assumption ultimately breaks down once significant portions of the reservoir have undergone bulk brittle failure (e.g. > ~50%) since this introduces variations in effective elastic stiffness over length scales comparable with the faults.

We determine brittle failure states within the reservoir according to the Griffith[15] stress criterion for tensile failure, and a Coulomb[16] stress criterion for shear failure. Whichever criterion is met first as the stress field changes determines the mode of first failure (Figure 4a).

Figure 4b shows one example of the distribution and type of brittle failure associated with the elastic stress field around the right-lateral strike-slip faults in Figure 2. Shear failure is predicted to localise around the fault tips whereas tensile failure occurs within the dilatational regions alongside faults.

The lateral extent of fractured regions depends on the rock strength relative to the remote driving stress: increased rock strength results in fractured areas shrinking towards the faults, and vice versa. We include fracture formation mechanisms such as fluid pressure increase, diagenesis, cooling, and erosion of the overburden as body forces, which produce an isotropic reduction in compressive stress within the calculations. This has the effect of shifting all the stress states plotted in Figure 4a towards the left and consequently increasing the lateral extent of both tensile and shear failure.

The a priori lateral extent of fractured areas is sometimes hard to predict, due to uncertainty in: (i) rock strength relative to the remote stress, and (ii) magnitude of body forces. Nonetheless the overall shapes of fracture clusters are far less uncertain as they correspond to contours of the elastic stress field. These depend only on fault geometry and the orientation of the remote stress, both of which are known. Consequently a small number of wells distributed across the field can provide sufficient data to validate the elastic stress field and constrain the lateral extent of fracturing.

Discrete fracture networks. Once the distribution and mode of failure has been determined the actual geometry of fracture networks responsible for permeability can be simulated by growing fractures in the brittle-elastic stress field. During growth, fracture spacing and interaction are controlled by a forbidden zone around each fracture - this represents an overall reduction in local stress due to the presence of the fracture. As a result other fractures are less likely to

nucleate within these zones, which limits the ultimate spacing of fractures. Furthermore, when the propagating tips of two fractures approach each other their mechanical interaction may lead to the fractures turning towards each other and connecting (fracture hooking)[17-19]. This is an important mechanism affecting fluid flow as it produces connectivity between essentially parallel fractures.

Figure 5 shows an example of a discrete tensile fracture network grown according to the stress field around the faults. Tensile fractures initiate in areas of tensile failure (Figure 4) and propagate in directions perpendicular to the orientation of least compressive stress in Figure 2b. Away from faults fractures propagate in the direction of regional stress, but close to the faults fractures grow along curved trajectories to become either parallel or perpendicular to the faults (c.f. Figure 3). This is a consequence of shear stress release on the faults and gives rise to variation in the direction of maximum fracture permeability close to faults.

The overall method described above for calculating elastic stress fields to predict the type and spatial distribution of brittle failure has been validated against an outcrop[14] at Nash Point, UK, where both faults and tensile fractures have been mapped in detail over an 80 m by 100 m area[20].

3. Flow simulation

Static fracture models can be calibrated and constrained locally, at the wellbore, with core data, image logs and mud losses. Calibration on a sector scale or field scale must be obtained through dynamic data, like well tests and history matching.

Well test simulation. Flow simulation of parts of the network without upscaling allows early selection of fracture models based on a comparison with well test data. Comparison of simulated well tests with actual results reduces the uncertainty in fracture permeability and lateral extent in the vicinity of the well.

To do this, we cut out regions of the fracture network model and simulate these without upscaling using MaficOil[21]. MaficOil is a finite-element simulator for single-phase flow through a three-dimensional fracture network. The matrix is discretised by three-dimensional tetrahedral elements and discrete fractures are represented by a parallel plate model at the faces of these elements. The fracture aperture and compressibility are inferred from geological data and then constrained by flow data. Matrix properties are obtained from sedimentological modelling programs like Geocap[22] or flow simulators like MoReS[23].

The simulated response of the well is then compared to actual data in standard well test evaluation programs. It often shows a pronounced reaction to all features of the fracture network: the anisotropy of individual fractures, the transition from fracture network to unfractured rock, and the diffusion of the pressure front into nearby fracture clusters. In real well tests wellbore storage may obscure the explicit response, but if the character of the simulation and field data is the same, well test simulations constrain the fracture model effectively on a sector scale.

Field scale simulation. Fracture models that have been constrained by well test simulations, are used for multi-phase simulation via dynamic upscaling to grid blocks. Shell's proprietary dual-permeability simulator MoReS[23] imports the hydraulic fracture properties via MaficOil, the program also used to simulate well tests. It computes the equivalent permeability of the fracture network within each grid block by flow simulation through the network inside the block (Figure 6). The upscaled fracture grid is then used to obtain a history match on field-scale, and to forecast development scenarios.

In addition to the effective permeability, several other static, parameters are computed: the number of matrix blocks in each grid block, the imbibition length, the permeability tensor etc. These parameters are used to check alignment of the simulator grid and fracture system, and to calculate static information like shape factors. Local grid refinement can be included.

MoReS itself adds dynamic properties like relative permeabilities and capillary pressures for matrix and fracture flow, to simulate multi-phase behaviour. Its comprehensive modelling capabilities allow simulation of complex, multi-phase recovery processes in heterogeneous dual-permeability systems. In our simple example the simulated interaction between water and oil results in dual-permeability behaviour of the reservoir (Figure 7). The fracture system connects a flank aquifer with a producer in the middle of the model, but water imbibition into the matrix delays water breakthrough. When the water cone in the fractures reaches the perforation after all, oil production must be cut back

4. Application to producing reservoirs

As an example results are shown for two producing carbonate reservoirs in the Shell Group: a tight, fractured carbonate oil reservoir, and a fractured, sour gas field with water encroachment. The oil reservoir contains highly overpressured, undersaturated oil, and is an example of a single-phase field under expansion drive. The gas reservoir represents a more complicated multiphase case.

A tight, fractured oil reservoir

This deep, Cretaceous oil field has an average matrix porosity less than 3% and an average matrix permeability less than 0.01 mD. An economically successful well in the reservoir must target a laterally extensive network of connected fractures to increase both the initial production rates and the ultimate recovery (UR). To help optimise well planning and reservoir development, the field-scale lateral distribution and hydraulic properties of the fracture systems were predicted using Poly3D, MaficOil and MoReS in combination (c.f. Figure 1).

The stress and fracture model. Fracture observations from core and outcrop analogues suggest a fault-related fracturing mechanism for the reservoir. Hence we interpreted fault geometries from 3D seismic data and calculated the elastic stress fields with Poly3D according to an orientation of remote palaeo-stress, determined by regional geological data. Brittle failure analysis of this stress field yields

a spatial probability distribution of tensile fracturing shown in Figure 8. These probabilities are derived according to uncertainty in rock strength over the field. The resulting fracture model is consistent with both fracture orientations and relative intensities as measured from image logs (UBI and CBIL) for 14 wells.

The calculated fracture map is significantly different to the common view that fault-related fractures are distributed as a simple function of distance to the nearest fault, producing a pattern of fracture halos around faults. Instead, the predicted fracture distribution shows large areas adjacent to faults which are essentially not fractured. Areas with sufficient effective fracturing are bound by faults but they tend to extend between rather than along them.

The history match. The fracture models that were grown according to the tensile fracture probability map, were upscaled dynamically via MaficOil. MoReS combined the resulting effective fracture permeability grids with upscaled matrix properties, to simulate the production history of the field. Dynamic validation of fracture models against production data from 10 wells proved to be a strong calibration of the approach.

In the simulation, wells were constrained by historical flowing bottom hole pressure data, whilst stimulations and mechanical integrity problems were modelled as a skin change. Figure 9 shows the simulated oil production rate versus cumulative oil produced, and the corresponding historical data. All plots have the same vertical scale, but the horizontal axis is different. The plots show that there are two classes of wells in the field: 1) wells that drain fracture clusters (top row) with high rates and an ultimate recovery that is effectively determined by fracture cluster size; and 2) wells located in unfractured regions (bottom row) with low rates, whose UR is determined by matrix properties alone. The middle row shows wells in fracture clusters that were stimulated, or that experienced integrity problems.

Our geomechanical fracture model, based on the fault interpretation, matches the (decline) rates in 9 out of the 10 producing wells, as well as pressure readings in observation wells, without any local parameter adjustment. The tenth well can be explained by refining the grid for both stress and flow calculations around this well. The extra resolution appears to be necessary to properly represent small-scale yet large stress perturbations associated with the junction of several nearby faults.

History matching a high proportion of wells greatly reduces the uncertainty in the fracture model away from the currently producing area. Indeed, several re-activations of old, shut-in wells since this work have confirmed the model, and production rates from all wells are, to date, consistent with the flow forecast.

Sensitivity analysis. Uncertainty in the orientation of remote stress, fault geometry and rock strength were all modelled via fracture network scenarios. The model described above is the only one out of the many considered that fits all static data and that gives a dynamic rate and pressure match. Changing either the rock strength or the body force magnitude, which affect the mode and lateral extent of fracturing, or the remote stress, which affects the shape of fractured areas, by more than 10% results in no more than four out of 10 wells showing a history match.

The results of these sensitivity studies demonstrate that both the location and lateral extent of the predicted fractured regions are required to explain both the static and dynamic data. A random distribution of fractured regions certainly does not suffice.

The value. Being able to predict fracture distribution and hydraulic properties on a field-scale has a clear business impact, as it increases the probability of success (POS) of a new well significantly. Wells located completely at random would have a probability of encountering a connected fracture system of just 0.3; wells at random near faults would have a POS of < 0.5. In contrast, field-wide fracture prediction increases the probability of locating economic fracture networks to 0.8–0.9. As a result the geomechanical fracture model shown here has become an integral part of further development planning.

A fractured gas field with water breakthrough. This example describes a carbonate field complex in Northern Germany, comprising a substantial part of BEB's sour gas reserves in that region. Since the field was put on-stream in the mid '80s it has been plagued by severe water problems.

The field. The carbonate complex consists of three communicating reservoirs that are heterogeneously fractured. Each reservoir consists of a dolomite package, sandwiched between two calcite layers. A layer with low matrix porosity and permeability is located in the centre of the dolomite package, and a highly permeable streak of some metres thickness sits between the top calcite and dolomite in only one part of the reservoir. Figure 10 shows the reservoir layout, and the well positions. The permeability of the matrix is typically less than 2 mD, except in the streak, where it can be as high as 5 D.

Water encroachment. Of the four wells experiencing water breakthrough, two did so in a most unusual way. These two wells sit in the Western part of the field, where the highly permeable streak runs near the top of one reservoir unit. Water advanced through this streak, but rained out into the fractures below before reaching the wells. Only after some years of production did this fractured matrix become so saturated that water finally entered the well perforations. The timing of water breakthrough in these wells depends on the volume of fractured rock below the streak. Elsewhere in the reservoir the highly permeable streak is absent, and water breakthrough occurs via coning of bottom water, if it occurs. Since water production has a high impact in a sour gas environment, knowledge of the fracture distribution and their flow properties is essential for field development.

Fracture prediction. In Northern Germany the regional stress evolution is well known[24], and the seismic data clearly show the faults (Figure 11), allowing us to follow the same route as in the previous example. The calculated stress field around the faults again determined the contours of fractured areas. The predicted lateral extent of these areas was then

constrained by varying the values of the rock strength and body force, to match data from FMIs, cores, well PIs and bottom hole pressure measurements.

History match. The simulated performance of the field not only depends on the extent of fracture networks, however, but also on the interaction of the fractures with the matrix. Fractures delay water breakthrough via the highly permeable streak by providing imbibition surfaces below the streak. The imbibition rate (i.e. the absorption of approaching water) depends on the fracture spacing, which must vary across the field to obtain a history match. By relating the fracture intensity to the calculated stress field, we computed the fracture spacing grid depicted in Figure 12, which gave a match in water breakthrough in the Western wells. Breakthrough in other wells, the tubing head pressures and reservoir pressure communication were subsequently matched by varying the aperture of the fractures (a single, field-wide parameter). Figure 13 shows the results for a typical well.

Sensitivity analysis. The requirement to match all geological and production data with a single geomechanical fracture model is a strong filter for subsurface scenarios. It constrained the match parameters in the predictive fracture model very effectively. For a given fault network and remote stress orientation these parameters are:
- relative rock strength and body force (2 numbers),
- fracture aperture (1 number), and
- fracture spacing versus stress intensity (1 number).

The range of these parameters that is consistent with all data is very narrow, and as a result the uncertainty in production forecasts can be reduced considerably.

The value. Indeed, the history matched simulation model now forms the basis for extensive field development planning. To this end, the MoReS model was coupled to a surface network simulator, describing the field's piping and facilities, such as separators, gathering centers, compressors etc. For each timestep in forecasting mode, this integrated Hydrocarbon Field Planning Tool (HFPT)[25] derives a solution for the pressure distribution within the surface network, and calculates the corresponding (multiphase) flow.

A snapshot of the surface network's pressure state is given in Figure 14. Apart from the wells producing from the carbonate reservoir, two other satellite fields feed gas to the delivery point. It is this point that puts a constraint on the network; be it a fixed delivery pressure, a contracted delivery rate or a certain gas quality requirement. The simulated offtake from the reservoir is controlled by opening or beaning back wells such that the network constraints and delivery requirements are fulfilled.

Because of its flexible surface network capabilities and the tight link to the subsurface reservoir simulator, HFPT offers a platform to quickly model various offtake scenarios and to evaluate the impact of future in-field measures, like timing of a drilling sequence, optimising pipeline debottlenecking (loops in the figure), design and timing of compressor units, economic screening of different gas contracts etc. In combination with the fractured reservoir simulation model, its relevance for BEB's integrated asset development has been increasing steadily.

5. Conclusions

In short, rocks obey physics, and physics can be used to predict fractures that affect flow across entire naturally fractured reservoirs.

Traditional methods of fracture modelling are geostatistical and somewhat different to the model described above. They rely on stochastic realisations of the large numbers of fracture networks consistent with borehole fracture data to explain inflow data. This approach is ultimately limited to near-well scales as it lacks information on how fracture statistics change away from wells. A field-scale stochastic fracture model would require an enormous number of evenly distributed wells to allow simple interpolation of fracture statistics between the wells.

The fracture model presented here uses geomechanical methods to predict the field-scale distribution of fractures that affect flow with reservoir simulations. Structural geometry governs the distribution of stress responsible for fracturing and can be used to constrain stress calculations (e.g. Poly3D). The field of stress determines the likely geometry and distribution of fracture networks which can be determined from models of fracture initiation, growth, and interaction. The lateral extent and permeability of fracture clusters are sensitive to uncertainties in both rock strength and hydraulic fracture aperture. These uncertainties can be significantly reduced using well test data and production history to validate and constrain flow simulations (MaficOil, and MoReS).

By modelling the physical processes responsible for fractures and flow more meaningful and realistic fracture systems can be predicted. Moreover, uncertainty can be minimised by integrating all the available static and dynamic data. As the model parameters are field-scale (i.e. mean rock strength, remote stress, etc.), information from each well constrains the whole fracture model and not just the areas close to wells. This makes the model suitable for fracture prediction and flow forecasting in all parts of the reservoir and not just those parts around existing wells.

Access to a predictive field-scale fracture model allows enhanced field development of naturally fractured reservoirs. Understanding and quantification of the fracture system helps to mitigate risks via improved flow forecasting, and optimal well placement and design.

Acknowledgements

This work benefited greatly through the involvement and ideas of Jean Borgomano, Tony Cortis, Arnout-Jan Everts, Karen Foster, Joel Ita, Bettina Kampman, Robin Leinster, Steve Livera, Thomas Mauduit, Dick Nieuwland, Steve Oates, Pascal Richard, Roeland Roeterdink. We thank Stanford University Rock Fracture Project for access to Poly3D.

References

1. Thomas, A.L. "Poly3D: A three-dimensional, polygonal element, displacement discontinuity boundary element computer program with applications to fractures, faults, and cavities in the Earth's crust." *Masters dissertation*, 1993, Stanford University, California 94305-2115.

2. Comninou, M.A., J. Dunders. "The angular dislocation in a half-space." *Journal of Elasticity*, **5** (1975) p. 216.
3. Jeyakumaran, M., J.W. Rudnicki, L.M. Keer. "Modeling slip zones with triangular dislocation elements." *Seismic Society of America Bulletin*, **82** (1992) p. 153-169.
4. Bürgmann, R., D.D. Pollard, S.J. Martel. "Slip distributions on faults: effects of stress gradients, inelastic deformation, heterogeneous host-rock stiffness, and fault interaction." *Journal of Structural Geology*, **16** (1994) p. 1675-1690.
5. Willemse, E.J.M., D.C.P. Peacock, and A. Aydin. "Nucleation and growth of faults in limestones from Somerset, UK." *Journal of Structural Geology*, 1997, p. 1461-1477.
6. Segal, P. and D.D. Pollard. "Mechanics of discontinuous faults." *Journal of Geophysical Research*, **85** (1980) p. 4337-4350.
7. Cowie, P.A., C.H. Scholtz. "Growth of faults by accumulation of seismic slip." *Journal of Geophysical Research*, **97** (1992) no. 1, p. 1085-1095.
8. Scholtz, C.H. N.H. Dawers, J.Z. Yu, M.H. Anders. "Fault growth and fault scaling laws: preliminary results." *Journal of Geophysical Research*, **98** (1993) p. 21,951-21,961.
9. Cowie, P.A., Z.K. Shipton. "Fault tip displacement gradients and process zone dimensions." *Journal of Structural Geology*, 1998, p. 983-997.
10. Aydin, A., R.A. Schultz. "Effect of mechanical interaction on the development of strike-slip faults with echelon patterns." *Journal of Structural Geology*, **12** (1990) p. 123-129.
11. Crider, J.G., D.D. Pollard. "Fault linkage: Three dimensional mechanical interaction between echelon normal faults." *Journal of Geophysical Research*, **103** (1998) no. 24, p. 373-391.
12. Pollard, D.D., P. Segall. "Theoretical displacements and stresses near fractures in rock: with applications to faults, joints, veins, dikes, and solution surfaces." In B.K. Atkinson (Ed.), *Fracture Mechanics of Rock*, 1987, Academic Press, London, p. 277-349.
13. Martel, J.S., W.A. Boger. "Geometry and mechanics of secondary fracturing around small three-dimensional faults in granitic rock." *Journal of Geophysical Research*, **103** B9 (1998) p. 21,299-21,314.
14. Bourne, S.J., E.J.M. Willemse. "Elastic stress control on the pattern of tensile fracturing around a small fault network at Nash Point, UK.", In prep.
15. Griffith, A.A. "The phenomena of rupture and flow in solids." *Philosophical Transactions of the Royal Society, London*, A 221, 1921, p. 163-198.
16. Coulomb, C.A. "Sur une application des règles de Maximis et Minimis a quelques problèmes de stratique relatifs à l'Architecture." *Académie Royal Des Sciences Memoires de mathématique et de physique par divers savans*, **7** (1773) p. 343-382.
17. Cruikshank, K.M., G. Zhao, A.M. Johnson. "Analysis of minor fractures associated with joints and faulted joints." *Journal of Structural Geology*, **13** (1991) no. 8, p. 865-886.
18. Olson, J.E., D.D. Pollard. "The initiation and growth of en échelon veins." *Journal of Structural Geology*, **13** (1990) no. 5, p. 595-608.
19. Thomas, A.L., and D.D. Pollard. "The geometry of echelon fractures in rock: implications from laboratory and numerical experiments." *Journal of Structural Geology*, **15** (1993) no. 3-5, p. 323-334.
20. Petit, J-P, V. Auzias, K. Rawnsley, T. Rives, in press. "Development of joint sets in association with faults." Georg Mandl Issue of *Lecture Notes for Earth Sciences*.
21. MaficOil. A special purpose version of Mafic. See: www.golder.com for a detailed description.
22. Taylor, S.R. "3D modelling to optimise production at the successive stages of field life", SPE 35501 (1996).
23. Boerrigter, P.M., L.E.C. van de Leemput, J. Pieters, K. Wit, J.G.J. Ypma. "Simulation of fractured reservoirs - case studies." SPE 26515 (1993).
24. Grote, R. "Maximum Horizontal Principal Stress Direction in Rotliegendes and Upper Carboniferous in North Germany." *Erdöl, Erdgas, Kohle*, **10** (1998).
25. Berkel, J. van, G. Kulawski, T. Schulte. "Integrated reservoir and surface network modelling in gas and oil fields using the hydrocarbon field planning tool." Accepted for publication in EuroPEC 2000, 24-25 October, Paris, France.

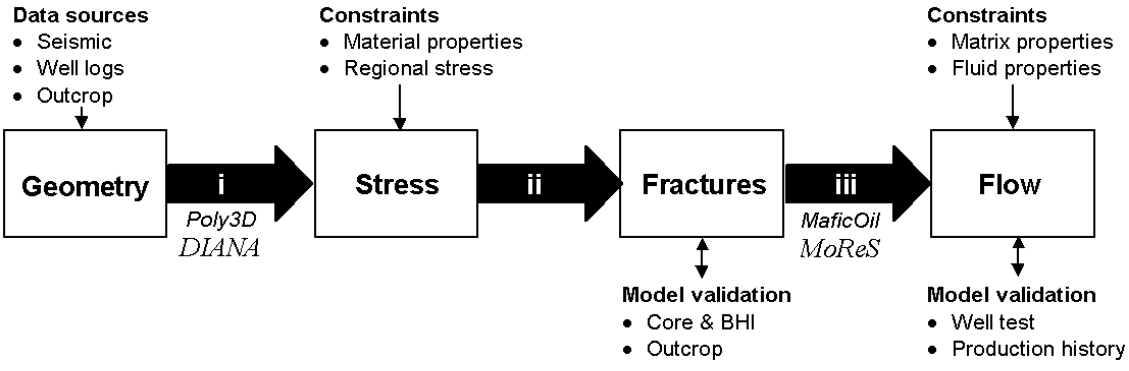

Figure 1. Integrated model for naturally fractured reservoirs based on: (i) geomechanical models of rock deformation, (ii) fracture mechanics, and (iii) multi-phase flow simulation. This workflow incorporates all the available static and dynamic data in order to constrain the model and minimise uncertainty in fracture prediction and flow forecasting.

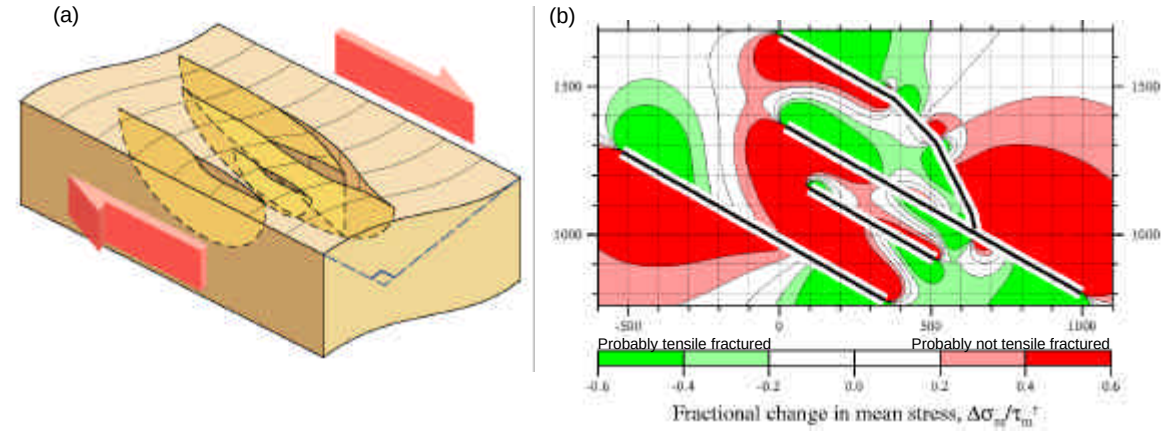

Figure 2. Example of an elastic stress field calculated for a three dimensional network of right-lateral strike-slip faults. The faults are triangulated and represented as surfaces of mechanical weakness. These are embedded in a linear elastic, isotropic, homogeneous rock body which is subject to a remote stress (a). The resulting stress field (b) is expected to govern the distribution of fault-related, small-scale tensile and shear fractures. Numerical solutions for the three-dimensional stress field were obtained using a boundary element method.

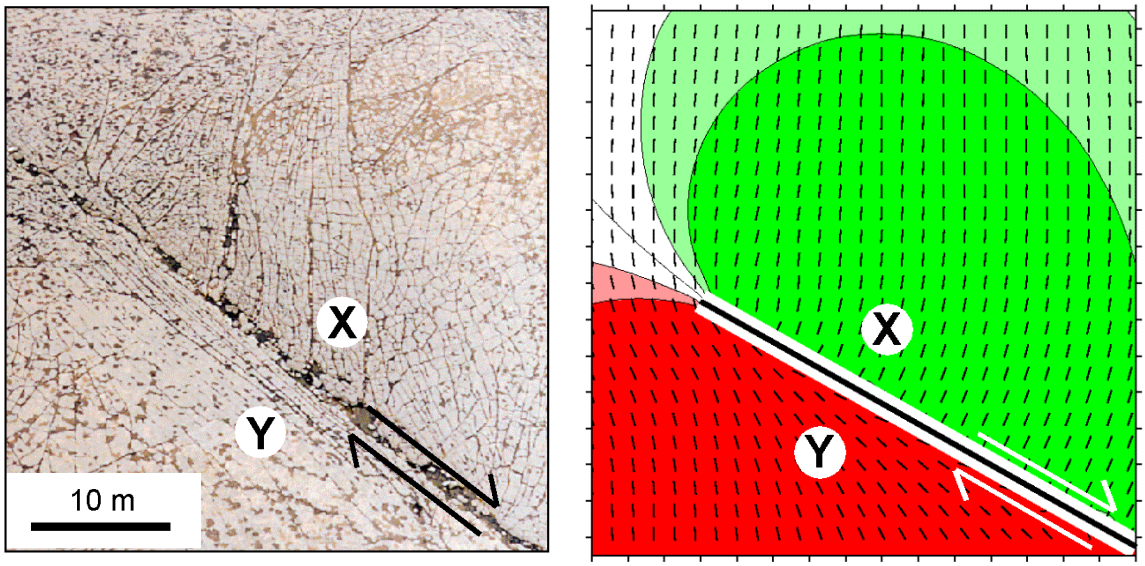

Figure 3. Distribution of tensile fractures around the tip of a strike-slip fault at Nash Point, Wales. Tensile fractures propagate in the direction of greatest compressive stress. At point X fractures propagate at high angles to the fault plane as rocks on that side of the fault have been stretched parallel to the fault by displacements away from the fault tip. Conversely, at point Y, rocks were displaced towards the fault tip increasing compression parallel to the fault and causing tensile fractures to propagate parallel to the fault.

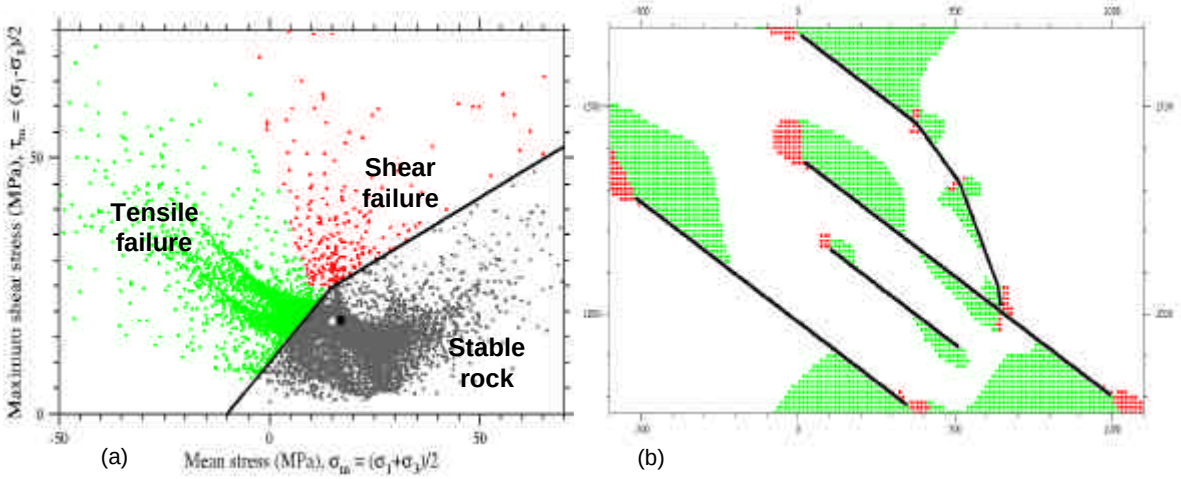

Figure 4. The extent and location of both tensile and shear fractures are calculated from the elastic stress field using the brittle failure strength of reservoir rock on the grid-block scale. In this case, secondary shear failure is confined to areas close to fault tips or kinks. Whereas tensile failure occurs over more extensive regions, bound on at least one side by a fault.

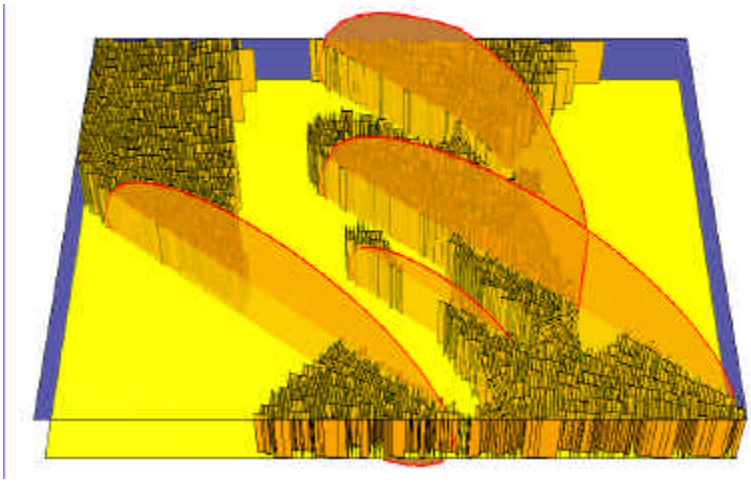

Figure 5. Example of a discrete fracture network obtained by simulating fracture growth according to the stress field calculated by Poly3D. Fractures initiate at points of brittle failure within the rock layer (Figure 4b) and propagate in directions determined by the local orientation of principal stress. Fractures terminate against each other or the large-scale faults. Fracture spacing is determined by the width of forbidden zones around each fracture within which other fractures cannot initiate because of a reduction in driving stress. Typically, fracture spacing would be about the thickness of the mechanical layer although in this figure the layer has been vertically exaggerated.

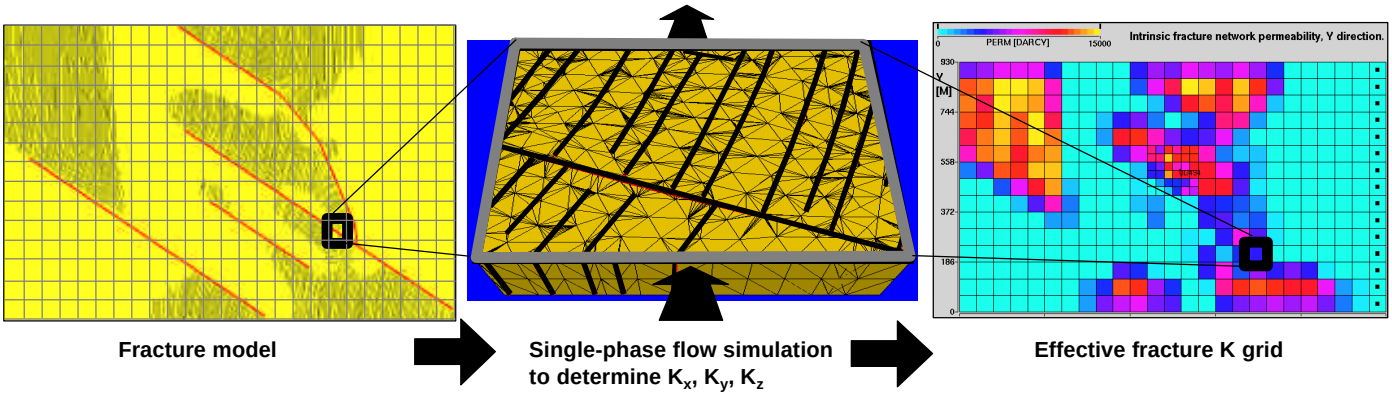

Figure 6. Dynamic upscaling of the fracture model to grid blocks of a dual porosity simulator. The equivalent permeability of the fracture network within each grid block is computed by flow simulation through the network inside the block in each direction.

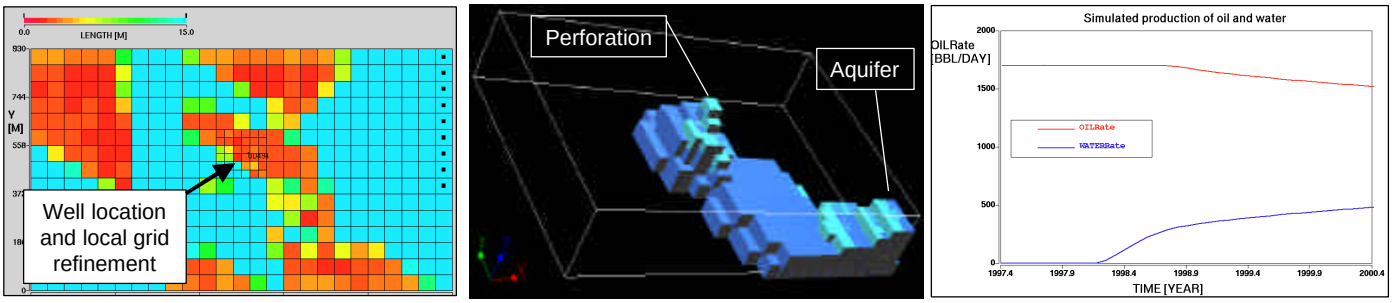

Figure 7. Multi-phase simulation of water encroachment through the fracture system. The well is shown as a circle in the aerial plot of the fracture spacing (left). The water cone advancing through the fracture network (middle) is delayed by imbibition into the matrix, but when it reaches the perforation after all, oil production must be cut back (right)

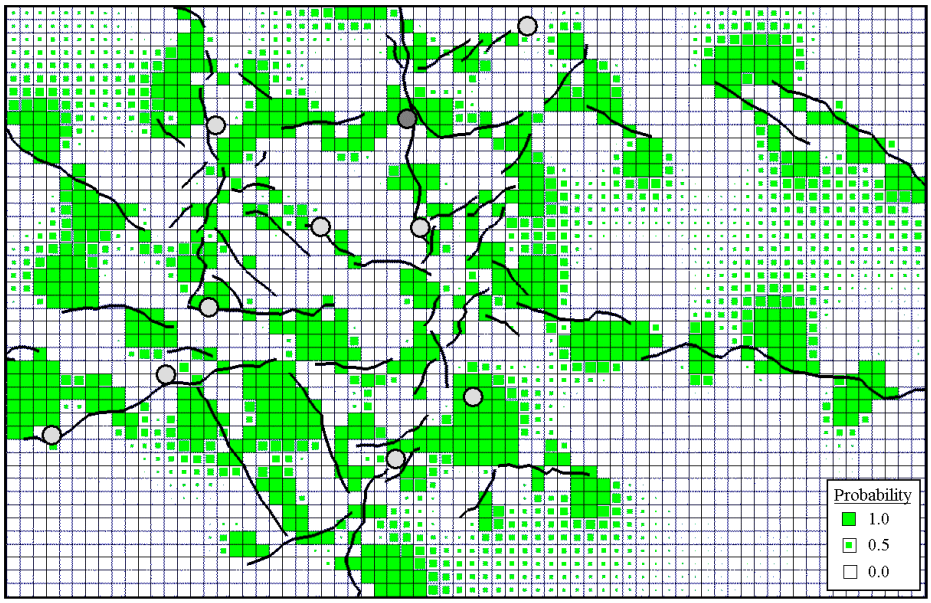

Figure 8. Map showing the spatial probability distribution of tensile fracturing in a producing carbonate field. This is based on the elastic stress field around the faults at the time of fracturing calculated using Poly3D. The location of ten producing wells are shown by circles and strike-slip faults are denoted in black. Areas of connected fractures are localised about, and sometimes extend between, the faults. Note that only some wells are connected to laterally extensive fracture networks. Grid block dimensions are 200 m by 200 m.

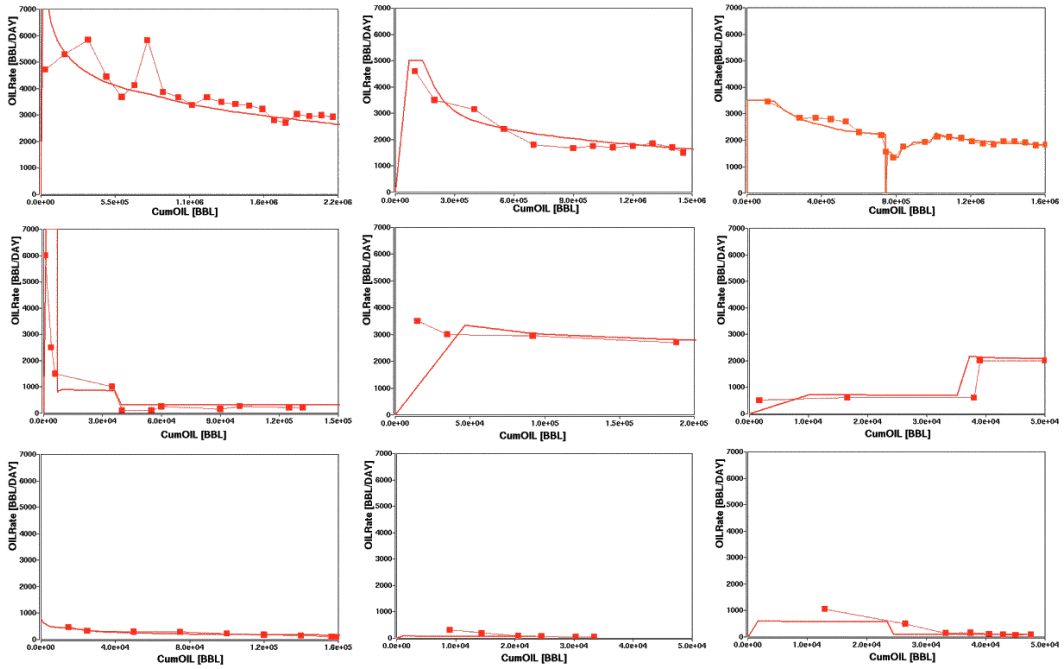

Figure 9. Simulated oil production rate (continuous line) versus cumulative oil produced, and the corresponding historical data (squares). All plots have the same vertical scale, but the horizontal axis is different. The simulated rates are generated by a single-phase, dual-permeability MoReS simulation, based on the fracture model from Figure 8 and an independent grid for matrix permeability.

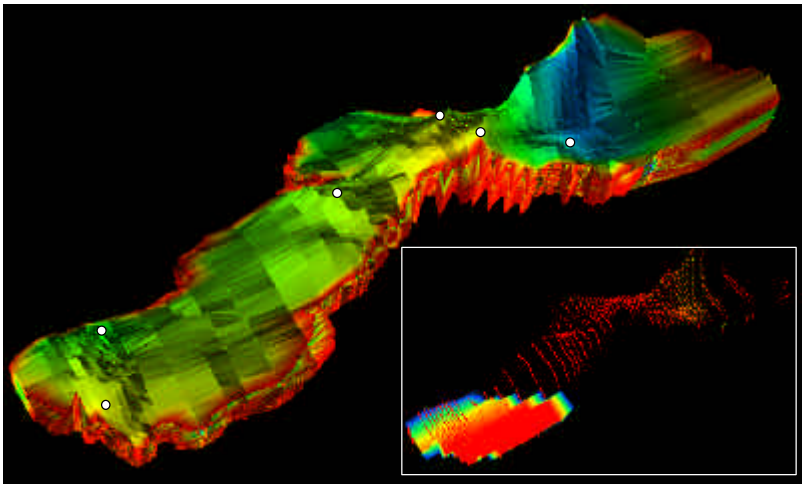

Figure 10. Three-dimensional view of matrix porosity in the fractured carbonate, sour gas field. The length and width of the field are about 18 by 5 km, and the vertical exaggeration is ten. The inset shows the highly permeable streak that occurs below the top calcite layer in one of the reservoirs. Circles indicate well positions.

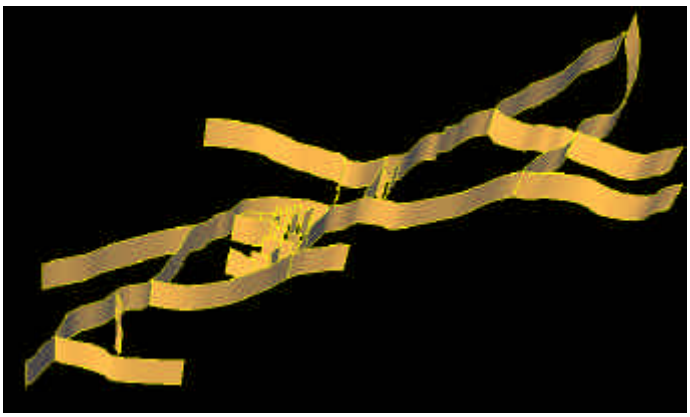

Figure 11. Vertical fault surfaces were extruded from interpreted fault traces to compute the stress perturbation resulting from fault slip in the field shown in Figure 10.

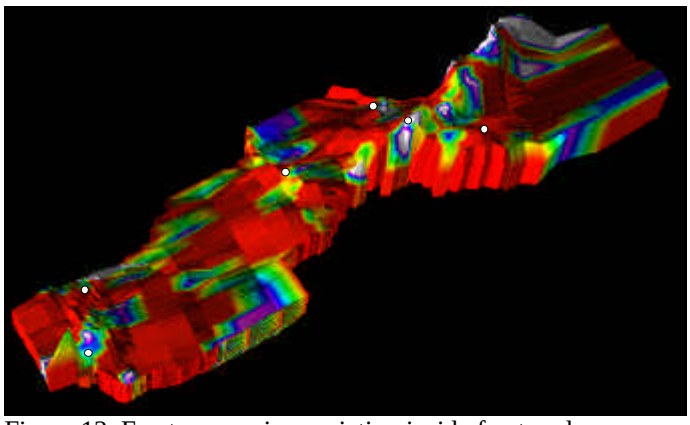

Figure 12. Fracture spacing variation inside fractured areas, based on brittle failure analysis of the calculated stress field around the faults in Figure 11. Fracture spacing determines the imbibition rate of water approaching through the fractures, influencing breakthrough times.

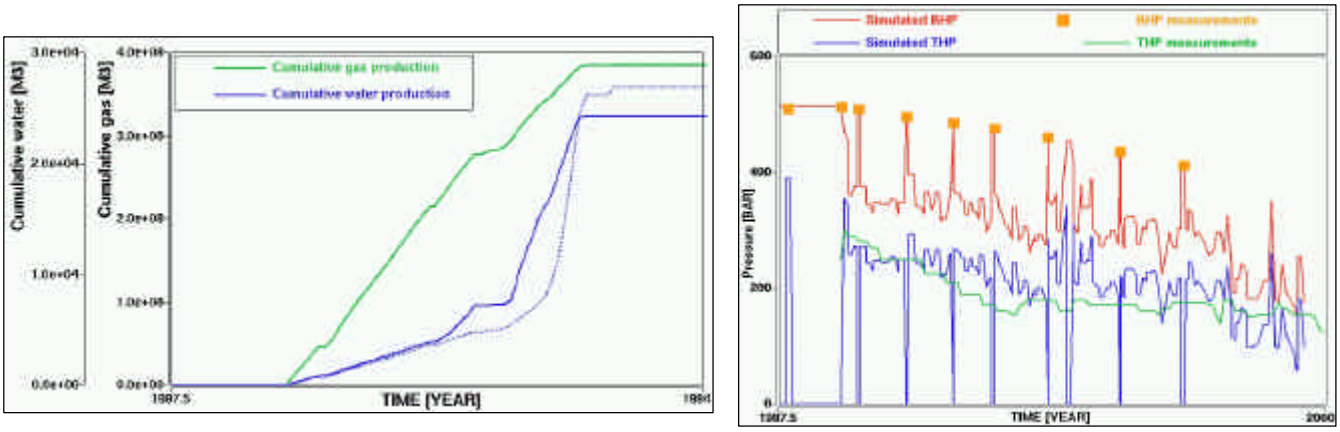

Figure 13. Simulated and historical production data (left) and pressure data (right) in one of the wells in Figure 10. Simulations were constrained via the cumulative gas production (historical and simulated data overlay each other). Formation water breakthrough (dashed = historical, continuous = simulated) shows up as a steep increase in the total water production (total = vapor + formation water). Bottom hole pressures (BHPs) are measured once every year during a close-in period, whereas tubing head pressures (THPs) are monitored on a continuous basis.

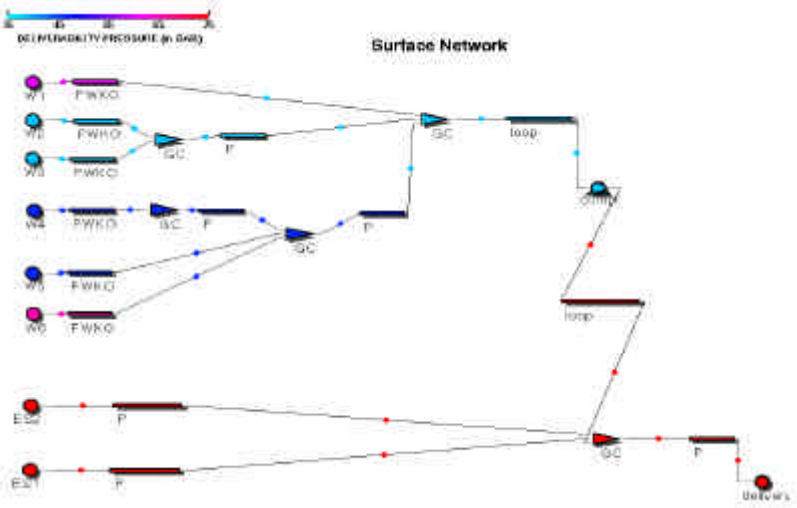

Figure 14. Snapshot of pressures in the surface network attached to the wells in Figure 10. Each of the wells (circles with W1 etc.) producing from the reservoir has its own free water knock-out unit (FWKO). Produced gas is fed via a pipeline system (P) and gathering centers (GC) to a compressor unit (comp). Further downstream two external sources (ES1,2) respresent two satellite fields, which also contribute to the resulting gas stream that eventually goes to the delivery point.